AD-A111 727 HUGHES RESEARCH LABS MALIBU CA F/G 20/2
MECHANISMS OF ISO-INDEX BEHAVIOR IN MATERIALS.(U)
FEB 82 J F LOTSPEICH, R C LIND N00014-80-C-0764
UNCLASSIFIED NL

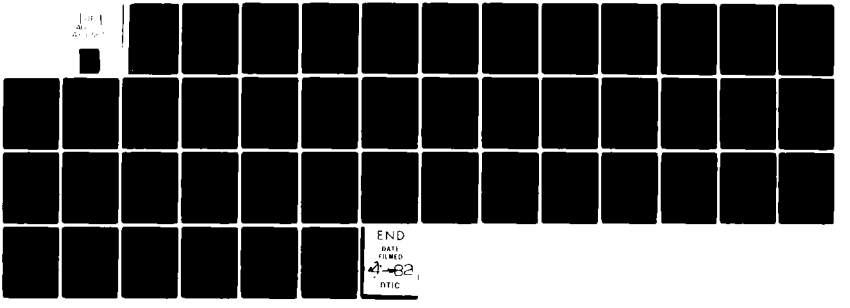

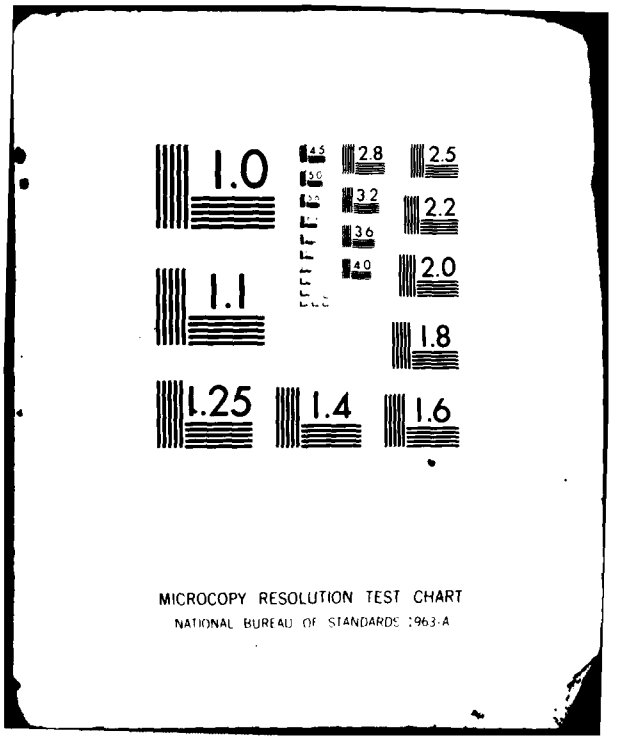
1.0
1.1
1.25
1.4
1.6
1.8
2.0
2.2
2.5
2.8
3.2
3.6
4.0
MICROCOPY RESOLUTION TEST CHART
NATIONAL BUREAU OF STANDARDS 1963-A

(12)

MECHANISMS OF ISO–INDEX BEHAVIOR IN MATERIALS

J.F. Lotspeich and R.C. Lind

Hughes Research Laboratories
3011 Malibu Canyon Road
Malibu, CA 90265

February 1982

N00014–80–C–0764
Final Technical Report
For Period 1 August 1980 through 31 December 1981

Approved for public release; distribution unlimited.

Prepared for
Office of Naval Research
800 N. Quincy Street
Arlington, VA 22217

SECURITY CLASSIFICATION OF THIS PAGE (When Data Entered)

REPORT DOCUMENTATION PAGE

READ INSTRUCTIONS BEFORE COMPLETING FORM

1. REPORT NUMBER	2. GOVT ACCESSION NO. AD-A111 727
3. RECIPIENT'S CATALOG NUMBER	
4. TITLE (and Subtitle) MECHANISMS OF ISO-INDEX BEHAVIOR IN MATERIALS	5. TYPE OF REPORT & PERIOD COVERED Final Report 1 Aug 1980 through 31 Dec 1981
	6. PERFORMING ORG. REPORT NUMBER
7. AUTHOR(s) J.F. Lotspeich and R.C. Lind	8. CONTRACT OR GRANT NUMBER(s) N00014-80-C-0764
9. PERFORMING ORGANIZATION NAME AND ADDRESS Hughes Research Laboratories 3011 Malibu Canyon Road Malibu, CA 90265	10. PROGRAM ELEMENT, PROJECT, TASK AREA & WORK UNIT NUMBERS
11. CONTROLLING OFFICE NAME AND ADDRESS	12. REPORT DATE February 28, 1982
	13. NUMBER OF PAGES
14. MONITORING AGENCY NAME & ADDRESS (if different from Controlling Office) Office of Naval Research 800 N. Quincy Street Arlington, VA 22217 Program Monitor: R.C. Pohanka	15. SECURITY CLASS. (of this report) UNCLASSIFIED
	15a. DECLASSIFICATION DOWNGRADING SCHEDULE

16. DISTRIBUTION STATEMENT (of this Report)

DISTRIBUTION STATEMENT A
Approved for public release;
Distribution Unlimited

17. DISTRIBUTION STATEMENT (of the abstract entered in Block 20, if different from Report)

Approved for public release; distribution unlimited.

18. SUPPLEMENTARY NOTES

19. KEY WORDS (Continue on reverse side if necessary and identify by block number)

Birefringent crystals, Iso-index characteristics, Dispersion theory, Blue-green filter design, Filter wavelength selection, Crystal synthesis presciption

20. ABSTRACT (Continue on reverse side if necessary and identify by block number)

This program entailed a theoretical study of the mechanisms in uniaxial crystals that give rise to a dispersion of the birefringence and in particular to the existence of an iso-index point, a wavelength at which the birefringence passes through zero and changes sign. This property has recently been exploited to devise highly selective optical filters for blue/green applications. The main thrust of the

DD FORM 1 JAN 73 1473 EDITION OF 1 NOV 65 IS OBSOLETE

UNCLASSIFIED

SECURITY CLASSIFICATION OF THIS PAGE (When Data Entered)

effort was to develop a mathematical tool for predicting the dispersive characteristics of the mixed alloy crystal $Zn_{1-x}Cd_xS$, based on knowledge of the refractive properties of the component binary crystals ZnS and CdS. The motivation was to prescribe iso-index points farther in the blue (~4700-4800 Å) than that of CdS near 5250 Å. Recognizing the impracticability of approaching the analysis on a first-principles basis, we adopted a phenomenological approach, taking the known values of the indices of CdS and ZnS and fitting them to a physically meaningful form, namely a sum of oscillators, wherein we might expect the parameters to vary linearly with fractional Zn content. Best results were obtained for both ordinary and extraordinary dielectric constants using a two-oscillator model, yielding calculations for indices typical within 0.2% of experimental data throughout the visible and near infrared wavelength range. For the mixed alloy system, our models for the most part correctly predicted a decrease in iso-index wavelength with increased Zn content but with only semiquantitative agreement with the limited data available. The most promising feature was a predicted corresponding increase in slope of birefringence, suggesting the possibility of enhanced filter selectivity toward the violet. A general conclusion was that experimental data is needed to obtain valid predictions on the refractive characteristics and iso-index filter potential of the (Zn,Cd)S alloys.

A

TABLE OF CONTENTS

LIST OF ILLUSTRATIONS

FOREWORD

This is the final technical report on Contract N00014-80-C-0764, Project NR 039-206. The work reported here was accomplished by Hughes Research Laboratories, a division of Hughes Aircraft Company, 3011 Malibu Canyon Road, Malibu, CA 90265. This research was accomplished during the period 1 August 1980 through 31 December 1981. The U.S. Navy program monitor was R.C. Pohanka, Code 471. This document was submitted on 28 February 1982. The principal investigator was J.F. Lotspeich and the program manager was R.C. Lind.

Significant contributions to the materials characterization and theoretical analysis presented in this report were made by D.M. Henderson, A.L. Gentile, and S.M. Wandzura of Hughes, and by Prof. T.C. McGill, Jr. of the California Institute of Technology. These contributions are gratefully acknowledged.

SECTION 1

INTRODUCTION AND SUMMARY

This report describes a theoretical research program to identify the mechanisms of iso-index behavior in materials, i.e., the crossover wavelength of the ordinary (n_o) and extraordinary (n_e) refractive indices in certain uniaxial crystals, where the birefringence ($n_e - n_o$) equals zero. Research of this nature could lead to an understanding and identification of candidate materials suitable for use in very wide field-of-view, very narrow bandwidth, optical filters for strategic laser communications in the blue/-green spectral region. An electro-optic filter designed at the Hughes Research Laboratories (HRL) relies on iso-index uniaxial crystals which, because of dispersion in the crystal birefringence, exhibit a zero crossing of birefringence at a specific wavelength known as the iso-index point. The iso-index phenomenon has been observed primarily in some of the II-VI compounds and ternary chalcopyrites of the type $A^{I}B^{III}C_2^{VI}$ which fall into hexagonal (including trigonal) or tetragonal crystal classes.

Our work in this area proceeds from an earlier Navy contract (N00014-78-C-0201) in 1978 to investigate new filter approaches to meet the challenging requirements of satellite-to-submarine communications. That study led to our concept of the iso-index coupled wave filter[1] in which polarized light is selectively coupled from the fast to the slow axes in those crystals exhibiting a zero crossing of birefringence. The calculated performance of this class of filters showed great promise for meeting blue/green requirements. For example, a filter of $AgGaS_2$, which has its iso-index point at 4970 Å, showed a calculated bandwidth of 0.3 Å over a full 2π sr FOV for a 1-cm interaction length.

On a subsequent program (N00014-79-C-0491), we fabricated test devices and demonstrated the narrow-bandwidth, wide-FOV properties offered by this technique. Specifically, our $AgGaS_2$ filters with 3-mm interaction length showed a 0.94-Å bandwidth.

The rapid progress in this area suggested that it was timely to attempt to determine those materials chat would allow this technique to be used at the candidate laser wavelengths of interest to blue/green programs. The general goals of this study effort were

- To understand the fundament properties of birefringent crystalline materials that lead to iso-index behavior.
- To develop the ability to predict the iso-index wavelength and filter bandwidth for new iso-index materials.

An important specific goal of this program was to provide the foundation for improved iso-index filters which operate at shorter wavelengths than currently possible (wavelengths from 4600 Å to 4800 Å are desired) and exhibit narrower bandwidths than are currently available (bandwidths as narrow as 0.1 Å are sought). Such filters would find immediate use in strategic laser communications.

The proposed methodology of the program was to determine energy level diagrams of known applicable materials of interest, determine polarization dependence and oscillator strengths of the bandgap transitions; then calculate iso-index and filter characteristics with no adjustable parameters for known materials, and finally predict new iso-index materials and their potential for narrowband filter applications.

In preliminary studes, we conceived and pursued a phenomonological model which, for known iso-index crystals, correctly predicted the location of the iso-index point and the strength of the dispersion at that location. This model recognized that the large dispersion in index of refraction near the band edge is responsible for the iso-index behavior. Subsequently we attempted to extend this work to include the quantum mechanical nature of the band-edge transitions so that the iso-index behavior could be predicted from first principles — a feature that was missing in the earlier theory. It soon became apparent, however, that it did not appear obvious that even the most highly refined first-principles theory would in fact prove universally tractable. Also, such an ambitious approach was well beyond the scope and capabilities as governed by time and funding constraints. We therefore decided to

proceed by refining our phenomenological theory. Using several different multiple-oscillator models, we showed that it is possible to predict the iso-index wavelength of CdS, for example, to within a fractional error of less than 0.10%. In addition, we demonstrated the capability to predict the ordinary and extraordinary refractive indices of ZnS over a broad range of visible and ultraviolet wavelengths to within a fractional error of less than 0.50%. ZnS, although not an iso-index material, is of practical interest to this program.

With the aim of developing an iso-index material having a cross-over wavelength farther into the blue than that of CdS (524.5 nm), we proposed to study the system $Zn_{1-x}Cd_xS$, since ZnS has a greater band gap than CdS but is nevertheless isomorphous with CdS. The reasoning was that adding a moderate amount of zinc would shift the dispersion curves closer to the blue while still preserving the iso-index characteristic. Moreover, there has been some experimental evidence that this does indeed occur over a limited compositional range. Our theory was based on a linear interpolation between the respective dielectric and band gap parameters of ZnS and CdS. At the present time, the theory appears to require further refinement. While predicting a monotonic decrease in wavelength of the iso-index point with increasing zinc concentration as anticipated, the theory does not agree quantitatively with the limited experimental data currently available.

In Section 2 we discuss some background considerations relevant to the theoretical approaches. Section 3 contains the development of our initial theoretical work based on a single classical oscillator model. This theory is further refined in Section 4 in which a more physically realistic multiple oscillator model is developed, leading to highly accurate values for the refractive index of CdS and ZnS over the whole range of visible wavelengths. In Section 5, an optional model based on the highly versatile Padé approximation to series solutions for the refractive indexes is put forth, yielding further insights into both the strengths and limitations of the theoretical models as applied to the Zn-Cs-S alloys.

SECTION 2

BACKGROUND THEORETICAL CONSIDERATIONS

In 1966, C.H. Henry[2] demonstrated an optical filter based on the sign change of the birefringence that occurs near the band edge in certain uniaxial semiconductors. He showed that light energy can be coupled between the ordinary and extraordinary polarization at the isotropic point by appropriately applied strain or magnetic field. Thus, when placed between crossed polarizers, the material acts as a narrowband filter. More recently, Laurenti[3] and coworkers demonstrated a filter tuning capability in mixed crystals of CdS and CdSe. At HRL, we have demonstrated how wave coupling can be achieved by an applied dc electric field, and we discovered a highly selective filter material, $AgGaS_2$, for the blue/green region.[1]

The iso-index phenomenon has been observed primarily in II-VI compounds[2] and ternary chalcopyrites[4] of the type $A^{I}B^{III}C_2^{VI}$. In addition, a few examples have been described, including a halide,[5] an oxysalt,[6] and an organic crystal,[5,7] all of which fall into the tetragonal or hexagonal (including trigonal) crystal classes. Known materials and their iso-index wavelength and crystal class are summarized in Table 1.

An examination of the theoretical explanation for the iso-index phenomenon introduces several concepts involving relationships to band gap,[4] compressional distortion,[4] and magnitude of the birefringence. Some of these concepts are discussed below. However, while a unified theoretical picture is beginning to emerge, none exists today that allows one to predict the iso-index properties of new crystals or existing birefringent crystals whose iso-index properties have not been characterized. One observation is the decrease in iso-index wavelength with increased band gap. We plan to use this relationship to tailor the blue/green filter currently under develoment for the 4600 to 4800-Å region (DARPA/ONR Contract No. N00014-81-C-0783). Nonetheless, at the current state of the art of related theory, we are unable to explain and predict: (1) whether a minimum band gap exists below which the crossover does not take place; (2) whether there is, therefore, a maximum iso-index wavelength attainable; and (3) what the required basic properties are to predict new materials.

Table 1. Iso-Index Crystals

9223-18 R1

CRYSTAL	DIRECT ENERGY GAP, eV	ISO–INDEX WAVELENGTH (Å, AT r.t.)	CRYSTAL CLASS POINT GROUP
$CuAlS_2$	3.5, 3.6, 3.6		TETRAGONAL $\bar{4}2M$
$CuAlSe_2$	2.7	>5000, <5500	TETRAGONAL $\bar{4}2M$
$CuGaS_2$	2.4, 2.6, 2.6	>6300, <6400	TETRAGONAL $\bar{4}2M$
$AgGaS_2$	2.7, 3.0, 3.0	4970 Å	TETRAGONAL $\bar{4}2M$
$AgInS_2$	1.9, 2.0, 2.0	?	TETRAGONAL $\bar{4}2M$
$AgGaSe_2$	1.8, 2.0, 2.3	~8040	TETRAGONAL $\bar{4}2M$
ZnO		~3960	HEXAGONAL 6MM
ZnS	3.6	<3600	HEXAGONAL 6MM OR 3M
CdS	2.4	~5240	HEXAGONAL 6MM
CdSe	1.8	~7060	HEXAGONAL 6MM
RINNEITE $K_3NaFeCl_6$		YELLOW	TRIGONAL 32
BENZIL $(CO{\cdot}C_6H_5)_2$		4200	HEXAGONAL (TRIGONAL) 32
TORBERNITE $Cu(UO_2)(PO_4)_2 \cdot 8H_2O$		5150	TETRAGONAL 4/MMM

The existence of different energy gaps in birefringent crystals for light polarized parallel ($\parallel$) and perpendicular ($\perp$) to the crystal's c axis is well known. It has become apparent that this property leads, under certain circumstances, to the iso-index effect. Such an example is shown in the electroreflectance data of Figure 1 for $AgGaSe_2$. The band-gap transition A shown in the inset of the figure occurs at the lowest energy and is predominantly excited by light whose electric field is parallel to the c axis. Transition B, which is different from A due to crystal field splitting, is higher in energy and predominantly excited by light polarized perpendicular to the c axis. We will refer to these two energy gaps as $E_\parallel$ and $E_\perp$. The parallel direction is associated with n_e (the index of refraction of the extraordinary ray), while the perpendicular direction is associated with n_o (the index of the ordinary ray).

The model used to describe the iso-index behavior is shown in Figure 2. The figure includes the possibility that $E_\parallel$ can be either $>E_\perp$ or $<E_\perp$ for both positive and negative uniaxial crystals. We have schematically shown both refractive indices as a function of frequency (ν) around the band gap. For simplicity, higher energy transitions have been ignored. An increase in index occurs because of resonance enhancement near the transitions. The birefringence $\Delta n = n_e - n_o$ is also shown in the figure. For positive uniaxial crystal ($\Delta n > 0$) at frequencies well removed from the band gap, it is clear that the iso-index point (denoted by ν_o) will exist only for $d\Delta n/d\nu < 0$. Thus, a necessary condition for the existence of an iso-index material is that the sign of the crystal birefringence must be opposite to the sign of the slope of the birefringence.

One group of materials whose birefringence is well characterized near the band gap is the ternay chalcopyrites. These materials have been thoroughly studied for nonlinear optical devices. Figure 3 shows the wavelength-dependent birefringence for 11 ternary compounds. The figure also shows the data for the II-VI semiconductor CdS and displays three of the four possible conditions for Figure 2. The following observations are noted:

- All the II-IV-V_2 crystals (underlined in Figure 3) are positive uniaxial with positive slope and therefore do not have an iso-index point.

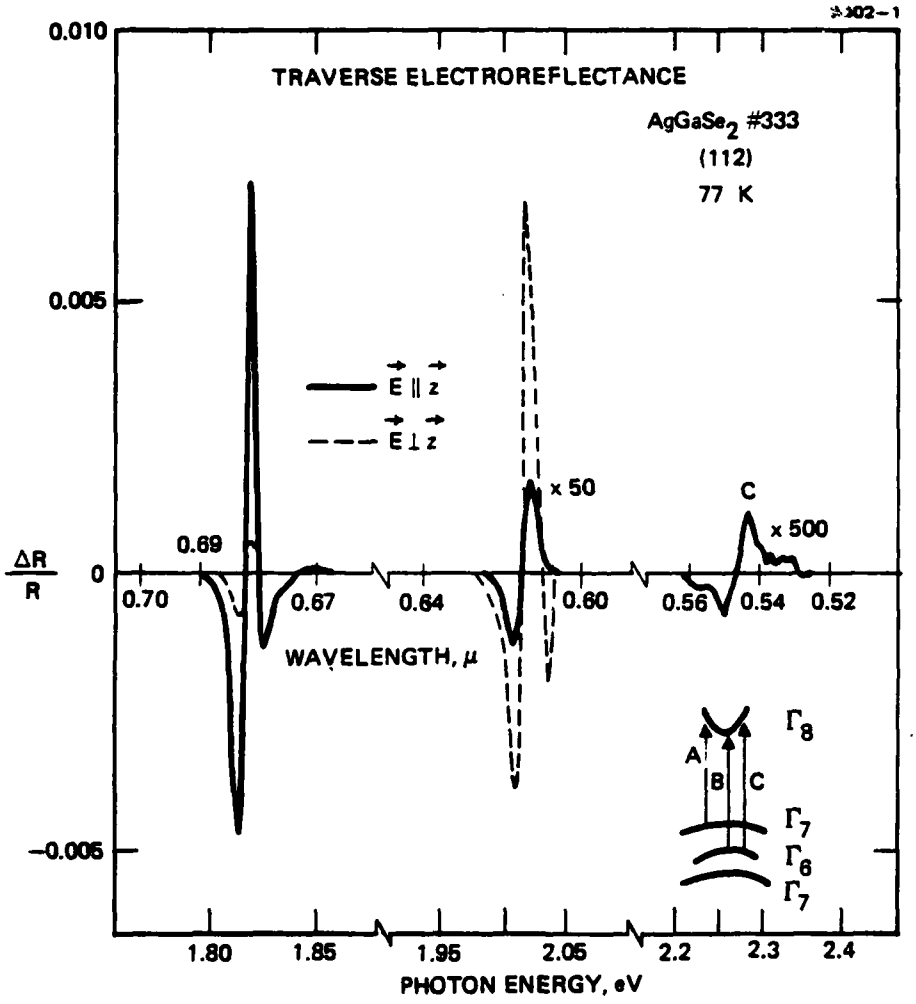

Figure 1. Electroreflectance spectrum of $AgGaSe_2$ (see Ref. 4).

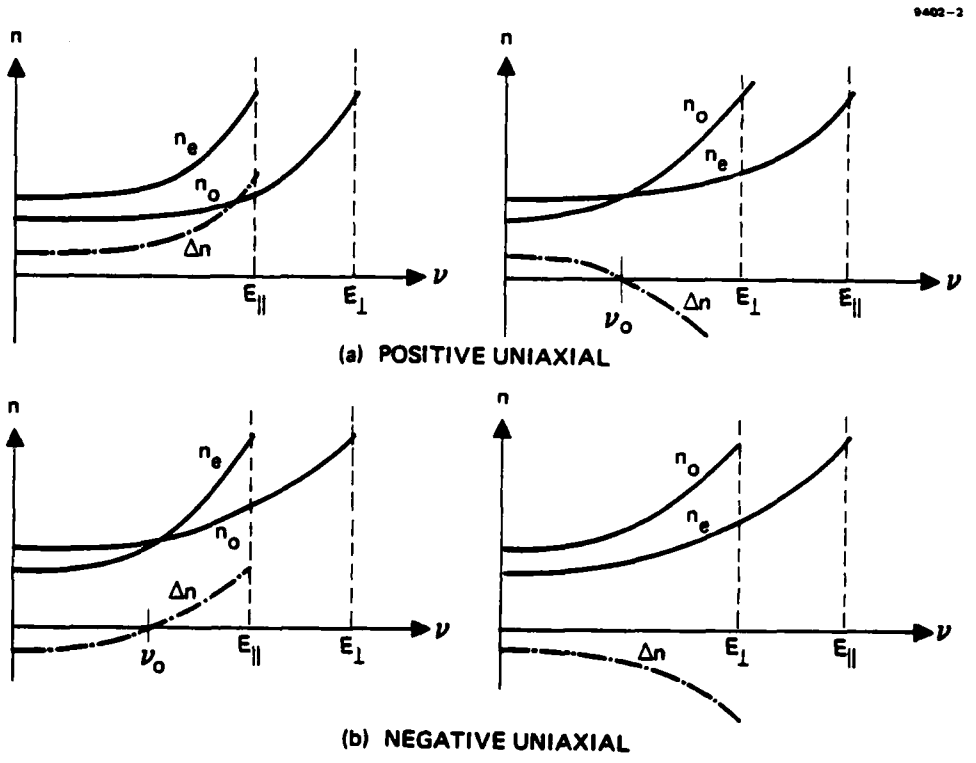

Figure 2. Dependence of birefringence ($\Delta n \equiv n_e - n_o$) on frequency in uniaxial crystals. The condition $E_\parallel < E_\perp$ is appropriate for ternary chalcopyrite semiconductors, while $E_\perp < E_\parallel$ is appropriate for binary II-VI semiconductors.

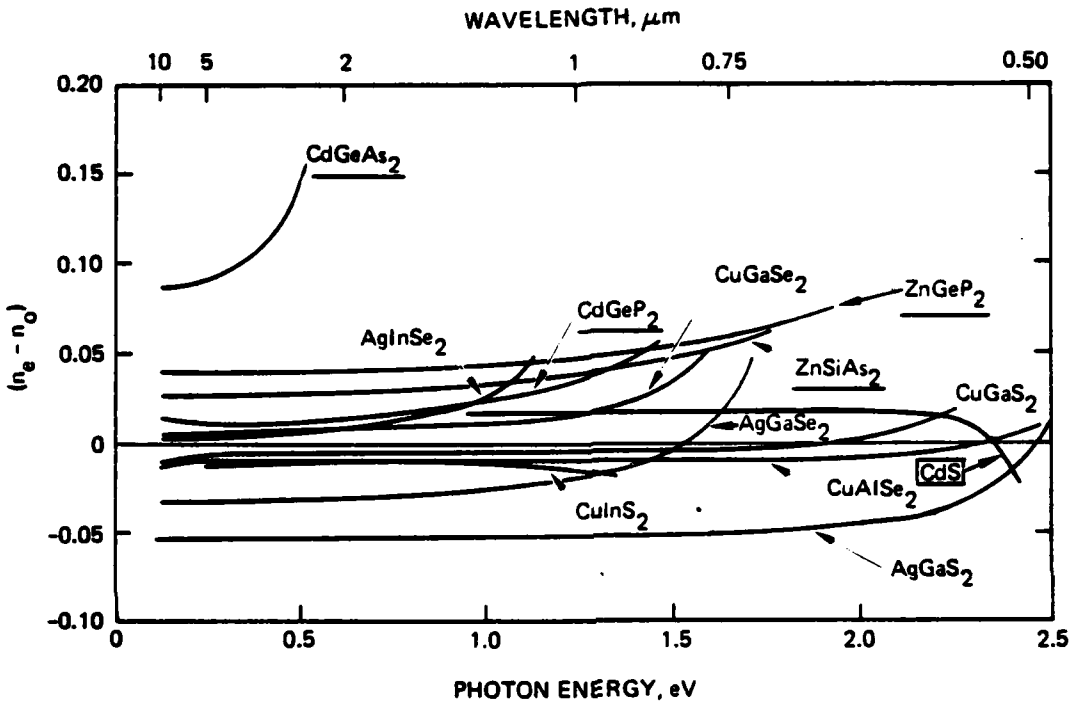

Figure 3. Birefringence of ternary chalcopyrites (taken from Ref. 4). The II-IV-V_2 compounds are underlined. Also shown is the binary II-VI semiconductor CdS.

- The I-III-VI_2 class contains both positive and negative uniaxial crystals. As expected, only those with a birefringence whose sign is opposite to that of the slope have iso-index points. In this case, they are all negative uniaxial. Electroreflectance data verifies that $E_{\parallel} > E_{\perp}$ for these crystals.

- An example of a positive uniaxial crystal with an iso-index point is the binary CdS. Electroreflectance data shows that $E_{\perp} > E_{\parallel}$ for this crystal.

- An example of a negative uniaxial crystal with no iso-index point is $CuInS_2$. However, low-temperature reflectance experiments show that the band gap transitions are polarization independent and so the model does not apply.

The model described by Figure 2 could be useful in selecting new materials according to the stated necessary conditions and provides the needed theoretical foundation for studying iso-index materials. The theory should include the variations in oscillator strength that are graphically implied in Figure 2. This will depend ultimately on the band structure of the semiconductors. The band structure is affected by the crystal field splitting of the valence p bonds, departure from cubic symmetry (compressional distortion), and higher lying transitions. An important, and perhaps the most challenging, goal is to gain an understanding of the change in iso-index behavior with compositional change that is needed to tailor iso-index material to specific laser wavelengths. In Figure 3, for example, the substitution of selenium for sulfur in $AgGaS_2$ shifts the $AgGaSe_2$ iso-index point to a longer wavelength, as expected. However, the entire character of the iso-index material $CuGaS_2$ is changed by substituting indium for gallium. In fact, $CuInS_2$ is not an iso-index material. Both are negative uniaxial crystals, but in this case the substitution has removed the polarization dependence, as discussed above.

SECTION 3

SINGLE OSCILLATOR MODEL

Preliminary theoretical calculations of the performance of iso-index filter materials based on the single oscillator model described in Section 2 yielded surprisingly good results in predicting the iso-index wavelength and the rate of change of birefringence with wavelength in the vicinity of the iso-index point.

We use the model to relate the slope in birefringence to optical properties near the band edge. This model is based on the following observations of known iso-index materials:

- There is a slight shift in the band edge between the ordinary and extraordinary directions of the crystal. This shift is seen in the reflection data of Figure 1.
- The index of refraction away from the band edge is larger for the orientation with the higher energy band edge.
- The iso-index point is fairly well removed from the band edge.

In calculating the iso-index point and its related slope, the last observation allows us to neglect the contribution to the index that arises from absorption. The first two lead to the model schematically shown in Figure 4. The refractive index of the higher energy orientation, indicated by the subscript 1, has the larger index of refraction away from the band edge. The parameters governing the iso-index point and its slope are $\varepsilon_1 - \varepsilon_2$ (recall the dielectric constant $\varepsilon \propto n^2$) and the shift in the band edge.

We now calculate the dependence of the zero-crossing and its related slope on the governing parameters. The dielectric constant of the materials is taken to have two contributions. Near the band edge, a resonant contribution arises from transitions at that wavelength. A constant, nonresonant background term is used to account for all remote transitions as their influence is slowly changing over the range of interest. Thus,

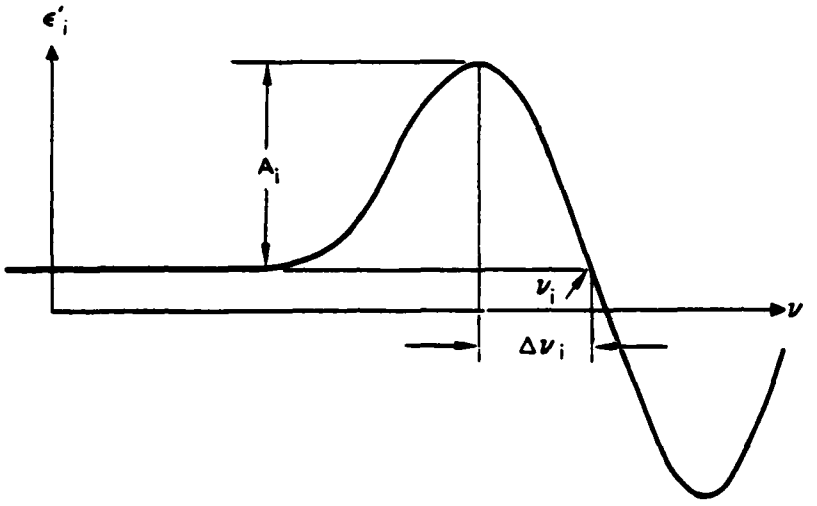

a) DEFINITION OF LINE SHAPE PARAMETERS

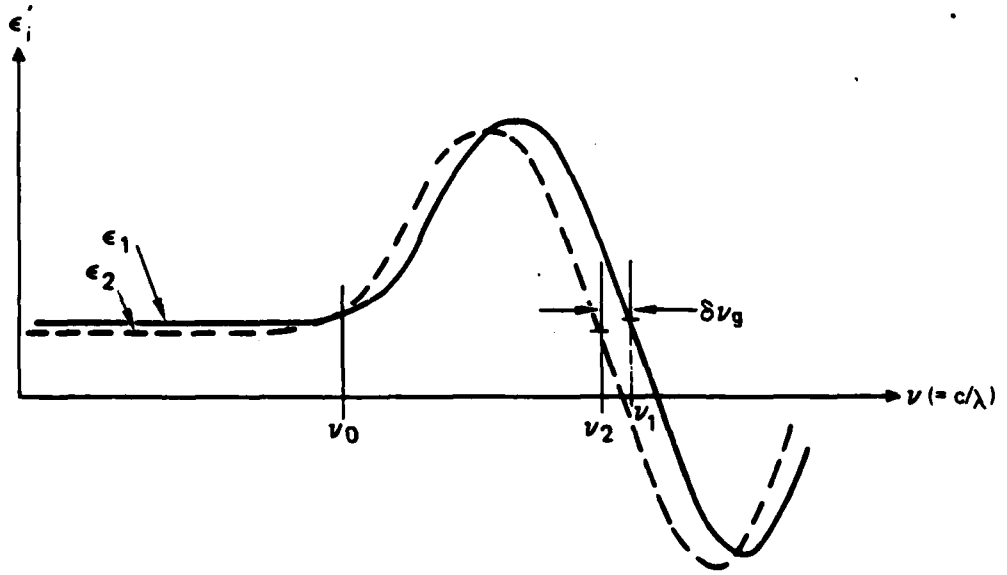

b) ISO-INDEX MODEL (ν_0 IS ISO-INDEX FREQUENCY)

Figure 4. Model for calculation of location of iso-index point and its slope.

$$\varepsilon_i'(\nu) = \varepsilon_i + \varepsilon_o \sum_j X_{ij}(\nu) \quad , \tag{3.1}$$

where i refers to the ordinary or extraordinary direction, ε_i is the non-resonant contribution, X_{ij} is the susceptibility of the j^{th} resonant transition near the band edge, and $\nu = c/\lambda$. The earlier observation that the iso-index point is fairly well removed from the band edge leads to yet another simplification. We use the Lorentzian lineshape of a classical oscillator* to describe the resonant transition. This lineshape becomes insensitive to the exact details of the linewidth and falls off as $1/\nu$ in the longer wavelength region. For the j^{th} transition, the susceptibility takes the form

$$X_{ij} = \frac{2\Delta\nu_{ij}A_{ij}(\nu_i - \nu)}{(\nu_i - \nu)^2 + \Delta\nu_{ij}^2} \simeq \frac{2\Delta\nu_{ij}A_{ij}}{(\nu_i - \nu)} \quad , \tag{3.2}$$

where the terms are defined in Figure 4. The parameter $\Delta\nu_{ij}A_{ij} \equiv f_{ij}$ is the oscillator strength of the j^{th} transition. Summing Equation (3.1) over the resonant transitions near ν_i gives

$$\varepsilon_i'(\nu) = \varepsilon_i + \frac{2F_i}{(\nu_i - \nu)} \quad , \tag{3.3}$$

where $F_i = \varepsilon_o \sum_j f_{ij}$.

We now calculate the dielectric constant difference between the two crystal directions:

$$\Delta\varepsilon = \varepsilon_i' - \varepsilon_2' = \varepsilon_1 - \varepsilon_2 + 2\left[\frac{F_1}{(\nu_1 - \nu)} - \frac{F_2}{(\nu_2 - \nu)}\right] \quad . \tag{3.4}$$

For simplicity, we assume that the oscillator strengths in the two directions are comparable and take $F_1 = F_2 = F$. The success of this model in predicting the zero-crossing and related slopes justifies this assumption, at least for the II-IV semiconductors and ternary chalcopyrite semiconductors studied. The iso-index point ν_o occurs at the zero of Equation (3.4), which gives

*This is an approximation applicable when $|\nu - \nu_i| \ll \nu_i$. The more exact form is shown in Equation (4.1) of Section 4.

$$(\bar{\nu}_g - \nu_o)^2 = \frac{2F\delta\nu_g}{\varepsilon_1 - \varepsilon_2} + \left(\frac{\delta\nu_g}{2}\right)^2 \simeq \frac{2F\delta\nu_g}{\varepsilon_1 - \varepsilon_2} , \tag{3.5}$$

where $\bar{\nu}_g = (\nu_1 + \nu_2)/2$ is the average band gap, and $\delta\nu = \nu_1 - \nu_2$ is the different in band gaps. The slope is obtained by differentiating Equation (3.4)

$$\left.\frac{d(\Delta\varepsilon)}{d\nu}\right|_{\nu=\nu_o} = 2F\left[\frac{1}{(\nu_1 - \nu_o)^2} - \frac{1}{(\nu_2 - \nu_o)^2}\right] = -\frac{4F\delta\nu_g(\bar{\nu}_g - \nu_o)}{[(\bar{\nu}_g - \nu_o)^2 - (\delta\nu_g/2)^2]^2} . \tag{3.6}$$

Then, by combining Equations (3.5) and (3.6) and again neglecting terms of order $(\delta\nu_g)^2$, we get

$$\frac{d(\Delta\varepsilon)}{d\nu} \simeq -\frac{2(\varepsilon_1 - \varepsilon_2)}{(\bar{\nu}_g - \nu_o)} . \tag{3.7}$$

Thus, the slope is nearly twice the difference in the dielectric constants divided by the separation of the zero-crossing from the mean band gap.

The slope of the birefringence Δn is related to that of Equation (3.7) by

$$\Delta\varepsilon = (n_1 + n_2)(n_1 - n_2) = 2\bar{n}\Delta n .$$

Consequently, Equations (3.5) and (3.7) become

$$(\lambda_o - \bar{\lambda}_g) \simeq \left(\frac{F}{c\bar{n}} \cdot \frac{\bar{\lambda}_g^2\delta\lambda_g}{n_1 - n_2}\right)^{1/2} \tag{3.8}$$

and

$$\frac{d(\Delta n)}{d\lambda} \simeq \frac{2(n_1 - n_2)}{\lambda_o - \bar{\lambda}_g} = \left[\frac{4c\bar{n}}{F} \cdot \frac{(n_1 - n_2)^3}{\bar{\lambda}_g^2\delta\lambda_g}\right]^{1/2} , \tag{3.9}$$

where again the subscripts o and g refer to the iso-index point and to the band gap, respectively; $\bar{\lambda}_g$ is the average band gap; and $\delta\lambda_g$ is the shift in band gaps.

We now proceed to calculate the zero-crossing and the slope of birefringence of several iso-index materials and to compare the values with measured quantities. Numerical values for the band-edge shift are obtained from reflection data such as those shown in Figure 1. The crystal birefringence $n_1 - n_2$ away from the band edge is taken from previous measurements such as those in Figure 3.

The measured offset of the iso-index point from the band edge for several II-VI semiconductors and ternary chalcopyrites is shown in Figure 5 along with the calculated offset from Equation (3.8). The agreement between theory and experiment in Figure 5 is ~±15%, which we feel is quite good considering that there is more than an order of magnitude variation in band gap splitting $\delta\lambda_g$ and birefringence $n_1 - n_2$ among the materials. The numerical value of the constant $(F/c\bar{n})^{1/2}$ of Equation (3.8), assumed approximately constant for all materials, was established by minimizing the deviation of the calculated curve. Thus, the factor containing the oscillator strength appearing in Equation (3.3) becomes

$$\frac{F}{c\bar{n}} = \frac{\Delta\nu_A}{c\bar{n}} = \frac{\Delta\lambda_A}{\lambda^2\bar{n}} = (1.6 \times 10^{-3})^2 \ . \qquad (3.10)$$

Evaluating this result at 5000 Å as an example gives $\Delta\lambda \cdot A = 160$ Å for $\bar{n} = 2.5$. Since $A \simeq 1$, this result shows that our model, which neglects the linewidth $\Delta\lambda$ of the transition, is consistent with the fact that $(\lambda_o - \lambda_g) \gg \Delta\lambda$.

In Figure 6, the measured slope is plotted against the parametric dependence of Equation (3.9). The measured slope varies by a factor of two at most from the calculated values over the range of three orders of magnitude of the horizontal axis. We believe that $AgGaSe_2$ shows the most disparity because it, unlike the other three, has an additional band edge transition not accounted for in the model (transition C of Figure 1).

The following general conclusions can be drawn from this work:

- Crystals with large birefringence are the best candidates for narrow-band filters.

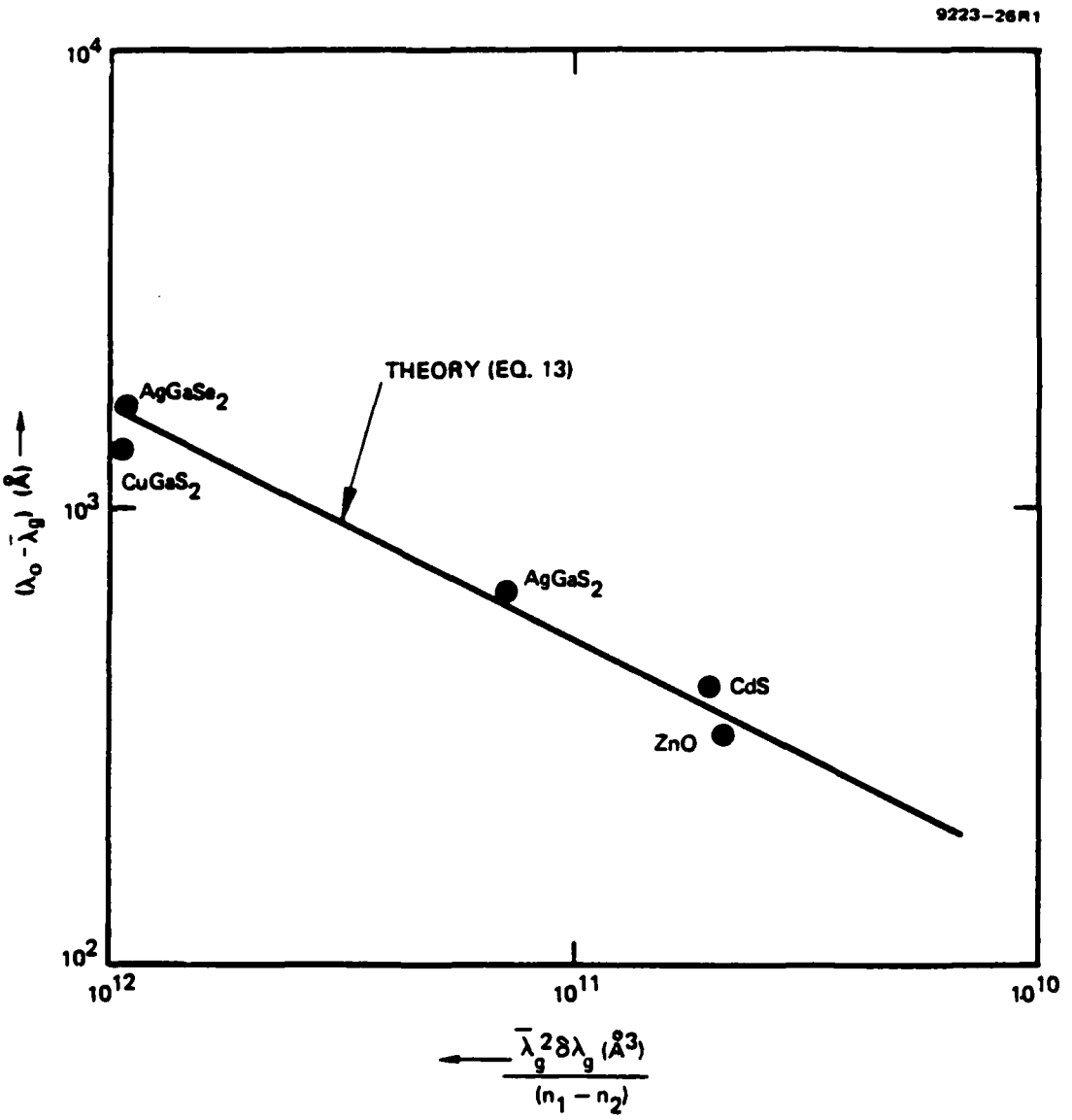

	$\bar{\lambda}_g$ (Å)	$\delta\lambda_g$ (Å)	$n_1 - n_2$	$\lambda_o - \lambda_g$ (Å)
ZnO	3637	48	0.013	323
$AgGaS_2$	4322	422	0.055	648
CdS	4834	38	0.017	411
$CuGaS_2$	4973	240	0.006	1341
$AgGaSe_2$	6429	686	0.030	1607

Figure 5. Measured offset of the iso-index point from band edge as function of material parameters.

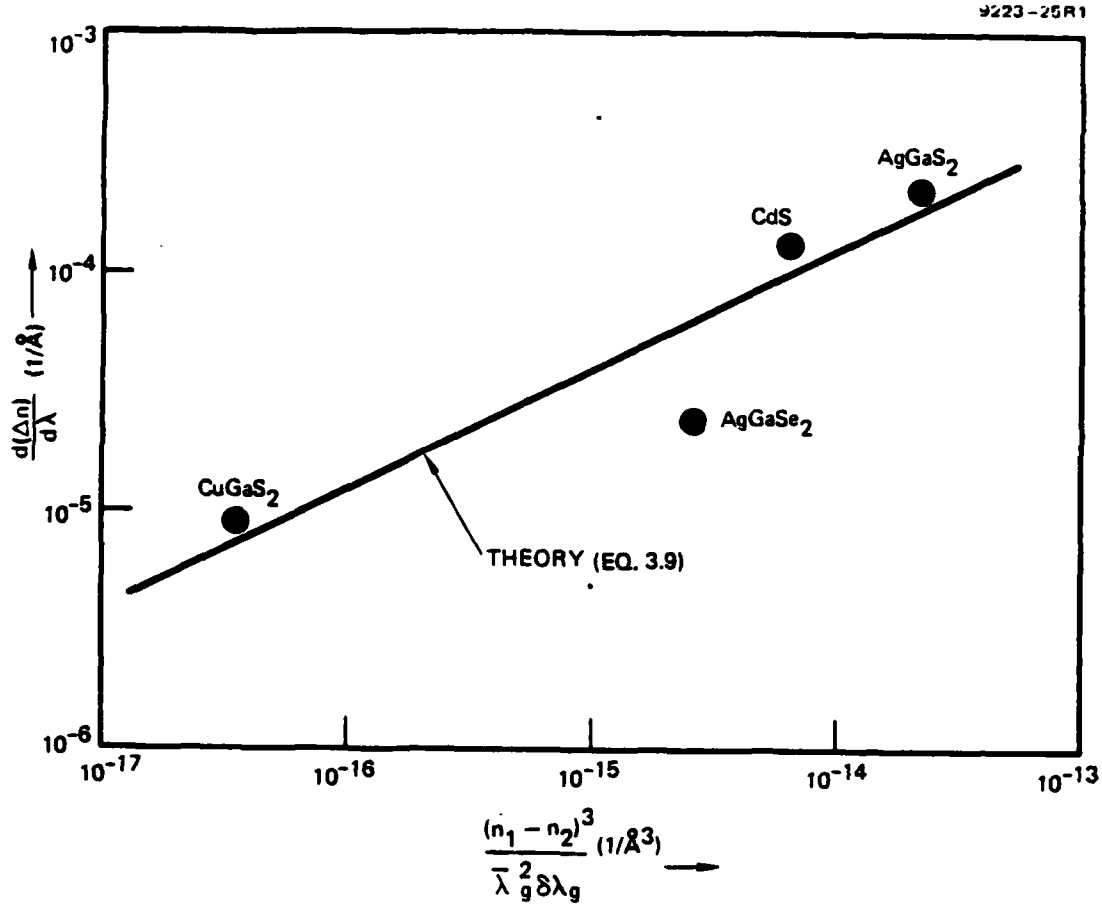

	$\bar{\lambda}_g$ (Å)	$\delta\lambda_g$ (Å)	$n_1 - n_2$	$d(\Delta n)/d\lambda$
$AgGaS_2$	4322	422	0.055	1.9×10^{-4}
CdS	4834	38	0.017	1.2×10^{-4}
$CuGaS_2$	4973	240	0.006	8.0×10^{-6}
$AgGaSe_2$	6429	686	0.030	1.9×10^{-5}

Figure 6. Measured slope at iso-index point as function of material parameters.

- Crystals such as II-VI semiconductors with smaller band-gap shifts are preferable if the crystal birefringence is sufficiently large.
- For comparable birefringence and band-gap shift, the shorter-wavelength filters offer narrower bandwidths.

The preceding comparison between results from the iso-index model and measurements gave us some confidence that the proposed model would provide the foundation for a more refined theoretical effort. The material presented in this section suggests that the following properties of candidate uniaxial crystals must be known in order to predict their iso-index behavior:

- Energy level diagram for at least the first two band-gap transitions
- Polarization properties of these transitions
- Oscillator strengths of these transitions
- Crystal birefringence (positive or negative uniaxial).

SECTION 4

MULTIPLE OSCILLATOR MODEL

This analysis was undertaken to investigate the properties of the indices of CdS, ZnS and their alloys $Zn_{1-x}Cs_xS$ to predict the iso-index point and the slope of the birefringence as a function of the composition (x). A number of different approaches are possible. One could attempt to predict the dielectric constants of CdS and ZnS from a band theory and then use the virtual crystal approximation on the alloy system to obtain predictions for the alloys. While in principle this approach is feasible, a review of the successes of the band theory in predicting the optical properties of these materials indicates that the success of this approach has not been such that we could expect to obtain the desired degree of accuracy for the dielectric constants.

A second approach is to take the known value of the indices[9] for CdS and ZnS and fit them to a physically meaningful form, where we might expect the parameters to vary linearly between the two cases in the alloys. This is the approach that we followed.

The form that seems most reasonable is the sum of oscillators

$$\varepsilon(\omega) = A(1) + \sum_{n=1} \frac{A(n+1)}{\omega(n)^2 - \omega^2 + \Delta\omega(n)^2} \quad . \tag{4.1}$$

In this equation, the A's and $\omega(n)$'s are obtained from fitting the known data.[9] As in Section 3, we neglect the terms $\Delta\omega(n)$ in the denominator since the frequencies of interest are well removed from the band edge. The symbology of Equation (4.1) differs from that of Section 3 but was used to conform to that of our computer print-outs displayed in the accompanying tables.

This approach was applied using one and two oscillators. (Trial results using more than two oscillators indicated no improvement in matching the formula to experimental data.) The results of fitting the data for CdS and ZnS are given in Tables 2 through 9. As can be seen, the fit using the single oscillator model can be off by nearly one percent while the calculation obtained by fitting the data with two oscillators is not off by more than 0.5% and is typically good to less than 0.2%. Hence, the two oscillator model gives a very good fit to the data.

Table 2. The Result of Fitting the Data for the Extraordinary Ray for CdS to the Single Oscillator Model. In the Table EXP. EP and TH. EP are Respectively the Experimental and Theoretical Values of the Dielectric Constants.

CdS Extraordinary Ray
A(1)= 0.44548D+01
A(2)= 0.71883D+01
W(1)= 0.28668D+01

WAVELENGTH(A)	FREQ.(eV)	EXP. EP	TH. EP	% ERROR
5120.	2.421	7.568	7.504	0.85
5130.	2.416	7.524	7.475	0.66
5140.	2.411	7.491	7.446	0.60
5150.	2.407	7.431	7.418	0.17
5160.	2.402	7.398	7.391	0.10
5170.	2.397	7.366	7.365	0.02
5180.	2.393	7.322	7.339	-0.22
5190.	2.388	7.301	7.313	-0.17
5200.	2.384	7.279	7.289	-0.13
5210.	2.379	7.258	7.265	-0.10
5220.	2.375	7.231	7.241	-0.14
5230.	2.370	7.209	7.218	-0.12
5240.	2.365	7.182	7.195	-0.18
5250.	2.361	7.156	7.173	-0.25
5275.	2.350	7.102	7.120	-0.25
5300.	2.339	7.044	7.070	-0.37
5325.	2.328	6.991	7.022	-0.45
5350.	2.317	6.954	6.976	-0.33
5375.	2.306	6.906	6.933	-0.39
5400.	2.295	6.875	6.892	-0.25
5425.	2.285	6.823	6.852	-0.44
5450.	2.274	6.791	6.815	-0.35
5475.	2.264	6.760	6.779	-0.28
5500.	2.254	6.724	6.744	-0.31
5750.	2.156	6.477	6.467	0.15
6000.	2.066	6.305	6.274	0.49
6250.	1.983	6.170	6.132	0.62
6500.	1.907	6.066	6.024	0.71
6750.	1.836	5.983	5.938	0.75
7000.	1.771	5.915	5.869	0.77
7500.	1.653	5.803	5.765	0.66
8000.	1.549	5.722	5.690	0.55
8500.	1.458	5.655	5.635	0.36
9000.	1.377	5.607	5.592	0.28
9500.	1.305	5.565	5.558	0.12
10000.	1.239	5.532	5.531	0.02
10500.	1.180	5.504	5.508	-0.08
11000.	1.127	5.476	5.489	-0.25
11500.	1.078	5.457	5.473	-0.30
12000.	1.033	5.438	5.460	-0.40
12500.	0.992	5.424	5.448	-0.44
13000.	0.953	5.410	5.438	-0.52
13500.	0.918	5.396	5.429	-0.61
14000.	0.885	5.387	5.422	-0.64

Table 3. The Result of Fitting the Data for the Ordinary Ray for CdS to the Single Oscillator Model. In the Table EXP. EP and TH. EP are Respectively the Experimental and Theoretical Values of the Dielectric Constants.

CdS Ordinary Ray
A(1)= 0.45217D+01
A(2)= 0.57794D+01
W(1)= 0.27850D+01

WAVELENGTH(A)	FREQ.(eV)	EXP. EP	TH. EP	% ERROR
5150.	2.407	7.524	7.465	0.78
5160.	2.402	7.480	7.432	0.65
5170.	2.397	7.437	7.399	0.50
5180.	2.393	7.388	7.368	0.26
5190.	2.388	7.339	7.337	0.02
5200.	2.384	7.301	7.308	-0.09
5210.	2.379	7.290	7.279	0.15
5220.	2.375	7.258	7.251	0.10
5230.	2.370	7.220	7.223	-0.04
5240.	2.365	7.188	7.196	-0.12
5250.	2.361	7.150	7.170	-0.28
5275.	2.350	7.081	7.108	-0.38
5300.	2.339	7.017	7.049	-0.45
5325.	2.328	6.959	6.994	-0.50
5350.	2.317	6.906	6.941	-0.51
5375.	2.306	6.849	6.892	-0.63
5400.	2.295	6.807	6.845	-0.56
5425.	2.285	6.770	6.801	-0.45
5450.	2.274	6.729	6.759	-0.44
5475.	2.264	6.693	6.718	-0.39
5500.	2.254	6.656	6.680	-0.36
5750.	2.156	6.391	6.380	0.16
6000.	2.066	6.215	6.178	0.59
6250.	1.983	6.086	6.033	0.87
6500.	1.907	5.983	5.925	0.98
6750.	1.836	5.890	5.840	0.86
7000.	1.771	5.827	5.772	0.94
7500.	1.653	5.712	5.672	0.70
8000.	1.549	5.636	5.601	0.62
8500.	1.458	5.574	5.548	0.47
9000.	1.377	5.522	5.508	0.26
9500.	1.305	5.480	5.476	0.07
10000.	1.239	5.448	5.451	-0.06
10500.	1.180	5.420	5.430	-0.19
11000.	1.127	5.401	5.413	-0.22
11500.	1.078	5.382	5.398	-0.29
12000.	1.033	5.364	5.386	-0.41
12500.	0.992	5.345	5.375	-0.55
13000.	0.953	5.331	5.366	-0.64
13500.	0.918	5.318	5.358	-0.75
14000.	0.885	5.308	5.351	-0.79

Table 4. The Result of Fitting the Data for the Extraordinary Ray for CdS to the Two Oscillator Model. In the Table EXP. EP and TH. EP are Respectively the Experimental and Theoretical Values of the Dielectric Constants.

CdS Extraordinary Ray
A(1)= 0.32103D+01
A(2)= 0.77818D+00
A(3)= 0.27471D+02
W(1)= 0.25675D+01
W(2)= 0.37713D+01

WAVELENGTH(A)	FREQ.(eV)	EXP. EP	TH. EP	% ERROR
5120.	2.421	7.568	7.560	0.11
5130.	2.416	7.524	7.518	0.07
5140.	2.411	7.491	7.479	0.16
5150.	2.407	7.431	7.442	-0.15
5160.	2.402	7.398	7.407	-0.12
5170.	2.397	7.366	7.374	-0.11
5180.	2.393	7.322	7.342	-0.26
5190.	2.388	7.301	7.311	-0.14
5200.	2.384	7.279	7.282	-0.03
5210.	2.379	7.258	7.253	0.06
5220.	2.375	7.231	7.226	0.06
5230.	2.370	7.209	7.200	0.12
5240.	2.365	7.182	7.175	0.10
5250.	2.361	7.156	7.151	0.06
5275.	2.350	7.102	7.094	0.11
5300.	2.339	7.044	7.042	0.03
5325.	2.328	6.991	6.993	-0.04
5350.	2.317	6.954	6.948	0.08
5375.	2.306	6.906	6.906	0.01
5400.	2.295	6.875	6.866	0.12
5425.	2.285	6.823	6.829	-0.10
5450.	2.274	6.791	6.794	-0.04
5475.	2.264	6.760	6.761	-0.01
5500.	2.254	6.724	6.729	-0.08
5750.	2.156	6.477	6.479	-0.03
6000.	2.066	6.305	6.305	0.01
6250.	1.983	6.170	6.173	-0.04
6500.	1.907	6.066	6.069	-0.04
6750.	1.836	5.983	5.984	-0.01
7000.	1.771	5.915	5.913	0.02
7500.	1.653	5.803	5.802	0.01
8000.	1.549	5.722	5.720	0.03
8500.	1.458	5.655	5.656	-0.01
9000.	1.377	5.607	5.605	0.05
9500.	1.305	5.565	5.564	0.02
10000.	1.239	5.532	5.530	0.04
10500.	1.180	5.504	5.501	0.04
11000.	1.127	5.476	5.477	-0.03
11500.	1.078	5.457	5.457	0.00
12000.	1.033	5.438	5.439	-0.02
12500.	0.992	5.424	5.424	0.00
13000.	0.953	5.410	5.411	-0.01
13500.	0.918	5.396	5.399	-0.05
14000.	0.885	5.387	5.388	-0.03

Table 5. The Result of Fitting the Data for the Ordinary Ray for CdS to the Two Oscillator Model. In the Table EXP. EP and TH. EP are Respectively the Experimental and Theoretical Values of the Dielectric Constants.

CdS Ordinary Ray
A(1)= 0.25833D+01
A(2)= 0.10270D+01
A(3)= 0.44825D+02
W(1)= 0.25567D+01
W(2)= 0.42872D+01

WAVELENGTH(A)	FREQ.(eV)	EXP. EP	TH. EP	% ERROR
5150.	2.407	7.524	7.525	-0.01
5160.	2.402	7.480	7.478	0.03
5170.	2.397	7.437	7.434	0.04
5180.	2.393	7.388	7.392	-0.06
5190.	2.388	7.339	7.352	-0.19
5200.	2.384	7.301	7.315	-0.19
5210.	2.379	7.290	7.279	0.15
5220.	2.375	7.258	7.245	0.18
5230.	2.370	7.220	7.212	0.11
5240.	2.365	7.188	7.181	0.10
5250.	2.361	7.150	7.151	0.00
5275.	2.350	7.081	7.081	0.00
5300.	2.339	7.017	7.018	0.00
5325.	2.328	6.959	6.960	-0.01
5350.	2.317	6.906	6.907	0.00
5375.	2.306	6.849	6.858	-0.13
5400.	2.295	6.807	6.812	-0.08
5425.	2.285	6.770	6.770	0.01
5450.	2.274	6.729	6.730	-0.02
5475.	2.264	6.693	6.693	0.00
5500.	2.254	6.656	6.658	-0.02
5750.	2.156	6.391	6.391	0.00
6000.	2.066	6.215	6.212	0.05
6250.	1.983	6.086	6.080	0.09
6500.	1.907	5.983	5.978	0.09
6750.	1.836	5.890	5.895	-0.07
7000.	1.771	5.827	5.826	0.03
7500.	1.653	5.712	5.718	-0.10
8000.	1.549	5.636	5.637	-0.02
8500.	1.458	5.574	5.574	0.01
9000.	1.377	5.522	5.524	-0.03
9500.	1.305	5.480	5.483	-0.06
10000.	1.239	5.448	5.450	-0.04
10500.	1.180	5.420	5.422	-0.04
11000.	1.127	5.401	5.398	0.05
11500.	1.078	5.382	5.378	0.09
12000.	1.033	5.364	5.360	0.07
12500.	0.992	5.345	5.345	0.01
13000.	0.953	5.331	5.331	0.00
13500.	0.918	5.318	5.320	-0.04
14000.	0.885	5.308	5.309	-0.02

Table 6. The Result of Fitting the Data for the Extraordinary Ray for ZnS to the Single Oscillator Model. In the Table EXP. EP and TH. EP are Respectively the Experimental and Theoretical Values of the Dielectric Constants.

ZnS Extraordinary Ray
A(1)= 0.34226D+01
A(2)= 0.37697D+02
W(1)= 0.46379D+01

WAVELENGTH(A)	FREQ.(eV)	EXP. E=	TH. EP	% ERROR
3600.	3.443	7.339	7.327	0.16
3750.	3.305	6.970	6.984	-0.21
4000.	3.099	6.574	6.588	-0.22
4100.	3.023	6.472	6.470	0.03
4200.	2.951	6.376	6.368	0.13
4250.	2.916	6.320	6.321	-0.02
4300.	2.883	6.275	6.278	-0.05
4400.	2.817	6.190	6.200	-0.15
4500.	2.754	6.136	6.130	0.09
4600.	2.695	6.066	6.068	-0.03
4700.	2.637	6.017	6.013	0.08
4750.	2.609	5.998	5.987	0.18
4800.	2.582	5.968	5.962	0.10
4900.	2.530	5.919	5.917	0.04
5000.	2.479	5.881	5.876	0.08
5250.	2.361	5.794	5.788	0.10
5500.	2.254	5.722	5.717	0.09
5750.	2.156	5.655	5.658	-0.06
6000.	2.066	5.607	5.609	-0.03
6250.	1.983	5.560	5.567	-0.13
6500.	1.907	5.522	5.532	-0.17
6750.	1.836	5.490	5.501	-0.20
7000.	1.771	5.462	5.474	-0.23
8000.	1.549	5.420	5.395	0.45
9000.	1.377	5.359	5.345	0.27
10000.	1.239	5.304	5.310	-0.11
12000.	1.033	5.262	5.267	-0.08
14000.	0.885	5.235	5.241	-0.12

Table 7. The Result of Fitting the Data for the Ordinary Ray for ZnS to the Single Oscillator Model. In the Table EXP. EP and TH. EP are Respectively the Experimental and Theoretical Values of the Dielectric Constants.

ZnS Ordinary Ray
A(1)= 0.34165D+01
A(2)= 0.37321D+02
W(1)= 0.46306D+01

WAVELENGTH(A)	FREQ.(eV)	EXP. EP	TH. EP	% ERROR
3600.	3.443	7.317	7.309	0.11
3750.	3.305	6.954	6.965	-0.16
4000.	3.099	6.554	6.568	-0.23
4100.	3.023	6.447	6.450	-0.05
4200.	2.951	6.360	6.347	0.20
4250.	2.916	6.305	6.301	0.06
4300.	2.883	6.260	6.258	0.03
4400.	2.817	6.180	6.180	0.01
4500.	2.754	6.116	6.110	0.09
4600.	2.695	6.047	6.048	-0.02
4700.	2.637	5.993	5.993	0.00
4750.	2.609	5.978	5.967	0.19
4800.	2.582	5.944	5.943	0.02
4900.	2.530	5.895	5.897	-0.04
5000.	2.479	5.861	5.856	0.09
5250.	2.361	5.770	5.768	0.02
5500.	2.254	5.693	5.697	-0.07
5750.	2.156	5.641	5.639	0.04
6000.	2.066	5.584	5.589	-0.10
6250.	1.983	5.541	5.548	-0.12
6500.	1.907	5.504	5.512	-0.16
6750.	1.836	5.471	5.482	-0.20
7000.	1.771	5.438	5.455	-0.31
8000.	1.549	5.401	5.376	0.46
9000.	1.377	5.336	5.326	0.19
10000.	1.239	5.295	5.291	0.06
12000.	1.033	5.244	5.248	-0.08
14000.	0.885	5.221	5.223	-0.03

Table 8. The Result of Fitting the Data for the Extraordinary Ray for ZnS to the Two Oscillator Model. In the Table EXP. EP and TH. EP are Respectively the Experimental and Theoretical Values of the Dielectric Constants.

ZnS Extraordinary Ray
A(1)= 0.33450D+01
A(2)=-0.19316D-02
A(3)= 0.40192D+02
W(1)= 0.34352D+01
W(2)= 0.46914D+01

WAVELENGTH(A)	FREQ.(eV)	EXP. EP	TH. EP	% ERROR
3600.	3.443	7.339	7.339	0.00
3750.	3.305	6.970	6.969	0.01
4000.	3.099	6.574	6.583	-0.14
4100.	3.023	6.472	6.467	0.07
4200.	2.951	6.376	6.366	0.15
4250.	2.916	6.320	6.321	-0.01
4300.	2.883	6.275	6.278	-0.05
4400.	2.817	6.190	6.200	-0.16
4500.	2.754	6.136	6.131	0.07
4600.	2.695	6.066	6.070	-0.05
4700.	2.637	6.017	6.014	0.05
4750.	2.609	5.998	5.989	0.15
4800.	2.582	5.968	5.964	0.06
4900.	2.530	5.919	5.919	0.00
5000.	2.479	5.881	5.878	0.04
5250.	2.361	5.794	5.790	0.06
5500.	2.254	5.722	5.719	0.05
5750.	2.156	5.655	5.660	-0.08
6000.	2.066	5.607	5.610	-0.05
6250.	1.983	5.560	5.568	-0.14
6500.	1.907	5.522	5.532	-0.18
6750.	1.836	5.490	5.501	-0.21
7000.	1.771	5.462	5.474	-0.23
8000.	1.549	5.420	5.394	0.46
9000.	1.377	5.359	5.343	0.30
10000.	1.239	5.304	5.308	-0.08
12000.	1.033	5.262	5.264	-0.03
14000.	0.885	5.235	5.238	-0.07

Table 9. The Result of Fitting the Data for the Ordinary Ray for ZnS to the Two Oscillator Model. In the Table EXP. EP and TH. EP are Respectively the Experimental and Theoretical Values of the Dielectric Constants.

ZnS Ordinary Ray
A(1)= 0.33631D+01
A(2)= 0.78449D-05
A(3)= 0.39029D+02
W(1)= 0.34431D+01
W(2)= 0.46681D+01

WAVELENGTH(A)	FREQ.(eV)	EXP. EP	TH. EP	% ERROR
3600.	3.443	7.317	7.317	0.00
3750.	3.305	6.954	6.955	-0.02
4000.	3.099	6.554	6.565	-0.18
4100.	3.023	6.447	6.448	-0.02
4200.	2.951	6.360	6.347	0.22
4250.	2.916	6.305	6.301	0.07
4300.	2.883	6.260	6.258	0.03
4400.	2.817	6.180	6.180	0.00
4500.	2.754	6.116	6.111	0.08
4600.	2.695	6.047	6.049	-0.04
4700.	2.637	5.993	5.994	-0.02
4750.	2.609	5.978	5.968	0.16
4800.	2.582	5.944	5.944	0.00
4900.	2.530	5.895	5.899	-0.06
5000.	2.479	5.861	5.858	0.06
5250.	2.361	5.770	5.770	0.00
5500.	2.254	5.693	5.698	-0.10
5750.	2.156	5.641	5.640	0.02
6000.	2.066	5.584	5.590	-0.12
6250.	1.983	5.541	5.549	-0.13
6500.	1.907	5.504	5.513	-0.17
6750.	1.836	5.471	5.482	-0.20
7000.	1.771	5.438	5.455	-0.31
8000.	1.549	5.401	5.376	0.46
9000.	1.377	5.336	5.325	0.21
10000.	1.239	5.295	5.290	0.09
12000.	1.033	5.244	5.246	-0.04
14000.	0.885	5.221	5.221	0.00

The results of calculating the iso-index point and slope of birefringence using a linear interpolation of the parameters are given in Table 10 for the two oscillator model and, for completeness, for the single oscillator model in Table 11. The results for the two oscillator model show that there are ranges of x where no iso-index point occurs. For other values of x, two iso-index points are found. For those x values where two iso-index points are found, the one with the smallest slope and the same sign for the slope as the other iso-index points is used. On comparing the results for two oscillators with those for a single oscillator, one can see that the results are very different even in the regions where both models give iso-index points. This fact militates to some degree against the validity of this approach.

The results for the iso-index point and slope for the two oscillator model are plotted in Figure 7. The data show a monotonically increasing value of the iso-index wavelength with increasing x. Some experimental data are available for the alloys.[3] These data also give a monotonically increasing value for the iso-index wavelength with incresing x. The data is approximately linear.

$$\lambda_{ISO}(x) = 3877 + 983x(\text{Å}) \text{ for } 0.4 < x < 0.7 \quad . \tag{4.2}$$

Our results are approximately linear over the same range but we obtain

$$\lambda_{ISO}(x) = 3460 + 1583x(\text{Å}) \text{ for } 0.40 < x < 0.7 \quad . \tag{4.3}$$

Hence, we differ by about 400 Å in the constant and almost a factor of two in slope.

This discrepancy remains an unsolved problem at this point. There is some doubt as to the accuracy of the experimental data given in Reference 3, but we have no way of quantifying this. With respect to our theoretical approach, we feel that pushing the empiricism as far as we have may not, in fact, be warranted. Reliable experiments are needed to yield valid information on the variation of the iso-index point with alloy composition.

Table 10. The Iso-Index Point and Slope as a Function of Composition for the Two Oscillator Model. WISO is the Iso-Index Frequency Measured in Electron Volts; LISO is the Iso-Index Wavelength Measured in A. DDn/Dw and DDn/DL are the Derivatives of the Difference in the Indices at the Iso-Index Point with Respect to Frequency and Wavelength, Respectively. The Parameters used are at the Top of the Table. The Range in which no Roots were Found is Measured in Electron Volts.

	CdSE	CdSO	ZnSE	ZnSO
A(1)=	.44548E+01	.45217E+01	.34226E+01	.34165E+01
A(2)=	.71883E+01	.57794E+01	.37697E+02	.37321E+02
W(1)=	.28668E+01	.27850E+01	.46379E+01	.46306E+01

Zn(1-x)Cd(x)S Dn=no-ne

X	WISO(eV)	LISO(A)	DDn/DW	DDn/DL
0.00	3.916	3164.9	.15182E-01	-.18787E-04
.05	3.549	3492.8	.90721E-02	-.92172E-05
.10	3.189	3887.1	.58489E-02	-.47981E-05
.15	2.817	4400.4	.37831E-02	-.24216E-05
.20	2.408	5148.0	.23203E-02	-.10852E-05
.25	1.910	6490.9	.12284E-02	-.36138E-06
.30	1.097	11297.7	.37562E-03	-.36477E-07
.35	NO ROOTS WERE FOUND IN .900 TO 3.985			
.40	NO ROOTS WERE FOUND IN .900 TO 3.892			
.45	NO ROOTS WERE FOUND IN .900 TO 3.800			
.50	NO ROOTS WERE FOUND IN .900 TO 3.708			
.55	NO ROOTS WERE FOUND IN .900 TO 3.615			
.60	NO ROOTS WERE FOUND IN .900 TO 3.523			
.65	NO ROOTS WERE FOUND IN .900 TO 3.431			
.70	1.439	8614.3	.18236E-02	-.30461E-06
.75	1.800	6885.2	.54364E-02	-.14214E-05
.80	2.006	6179.1	.11862E-01	-.38506E-05
.85	2.144	5782.0	.23328E-01	-.86488E-05
.90	2.242	5529.6	.44286E-01	-.17952E-04
.95	2.313	5359.8	.84501E-01	-.36460E-04
1.00	2.364	5242.8	.16844E+00	-.73959E-04

Table 11. The Iso-Index Point and Slope as a Function of Composition for the Single Oscillator Model. WISO is the Iso-Index Frequency Measured in Electron Volts; LISO is the Iso-Index Wavelength Measured in A. DDn/Dw and DDn/DL are the Derivatives of the Difference in the Indices at the Iso-Index Point with Respect to Frequency and Wavelength, Respectively. The Parameters used are at the Top of the Table. The Range in which no Roots were Found is Measured in Electron Volts.

	CdSE	CdSO	ZnSE	ZnSO
A(1)=	.32103E+01	.25833E+01	.33450E+01	.33631E+01
A(2)=	.77818E+00	.10270E+01	.00000E+01	.78449E-05
A(3)=	.27471E+02	.44825E+02	.40192E+02	.39029E+02
W(1)=	.25675E+01	.25567E+01	.34352E+01	.34431E+01
W(2)=	.37713E+01	.42872E+01	.46914E+01	.46681E+01

Zn(1-x)Cd(x)S Dn=no-ne

X	WISO(eV)	LISO(A)	DDn/DW	DDn/DL
0.00	NO ROOTS WERE FOUND IN .900 TO 3.435			
.05	NO ROOTS WERE FOUND IN .900 TO 3.392			
.10	NO ROOTS WERE FOUND IN .900 TO 3.348			
.15	NO ROOTS WERE FOUND IN .900 TO 3.305			
.20	NO ROOTS WERE FOUND IN .900 TO 3.262			
.25	3.181	3896.3	.40873E+00	-.33371E-03
.25	3.203	3870.1	-.20198E+01	.16715E-02
.30	3.126	3964.5	.51682E+00	-.40758E-03
.35	3.074	4032.2	.55340E+00	-.42188E-03
.40	3.022	4101.4	.56713E+00	-.41789E-03
.40	3.087	4015.5	-.49425E+03	.37994E+00
.45	2.970	4172.9	.56572E+00	-.40269E-03
.50	2.919	4246.9	.55597E+00	-.38208E-03
.55	2.867	4323.9	.53927E+00	-.35752E-03
.60	2.814	4404.3	.51713E+00	-.33044E-03
.65	2.762	4488.4	.49135E+00	-.30231E-03
.70	2.708	4577.1	.46002E+00	-.27217E-03
.75	2.654	4670.5	.42698E+00	-.24261E-03
.80	2.599	4769.8	.39110E+00	-.21308E-03
.85	2.542	4875.8	.35316E+00	-.18413E-03
.90	2.484	4989.6	.31421E+00	-.15644E-03
.95	2.424	5113.1	.27449E+00	-.13014E-03
1.00	2.361	5248.9	.23416E+00	-.10534E-03

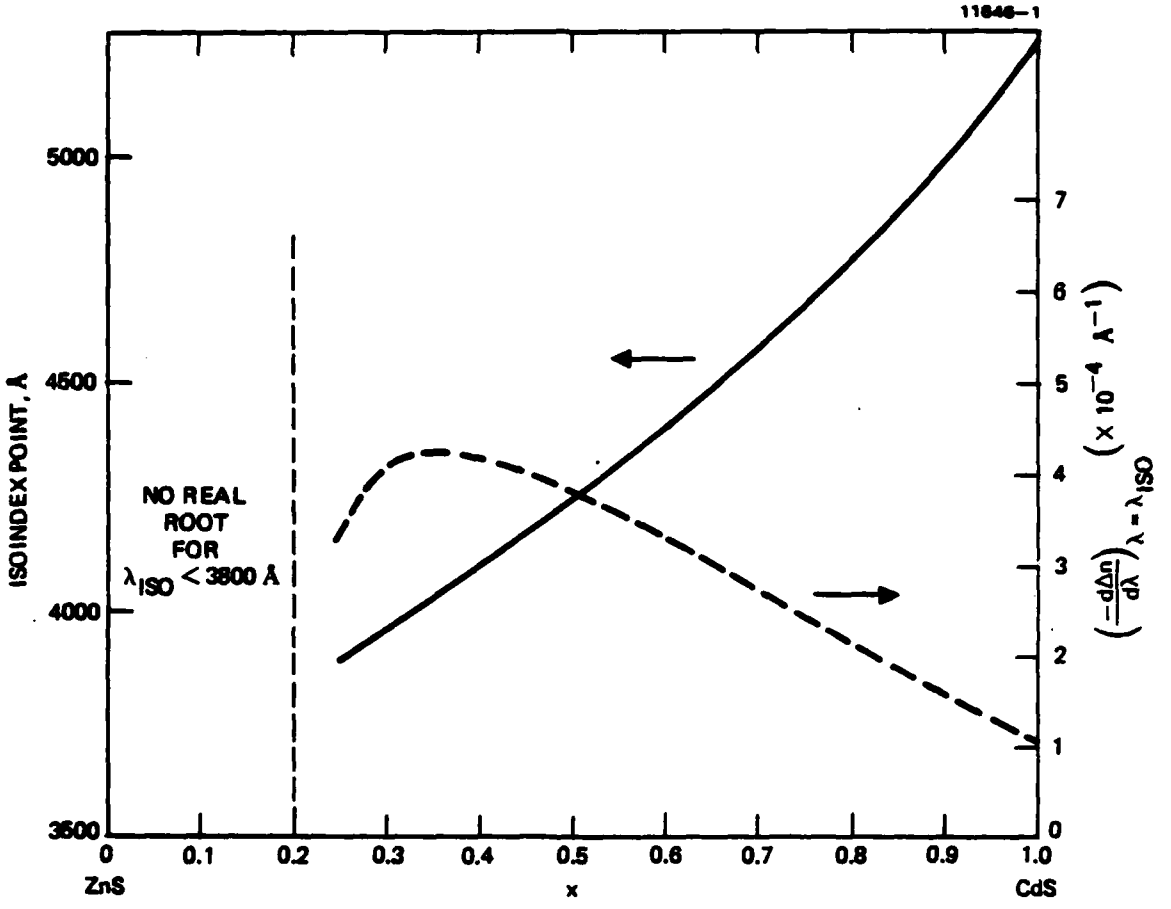

Figure 7. The iso-index wavelength and the slope of the difference between the indices at the iso-index point as a function of alloy composition.

SECTION 5

THE PADÉ APPROXIMATION

The Padé approximation is a very useful and powerful method for representing any analytic function (which is more traditionally represented by an infinite series) in terms of a quotient of two series, usually of much more limited order. Since the real part of the refractive index is an analytic function of the frequency squared[10] (ω^2), we attempted to fit the four indices of refraction of CdS and ZnS tabulated by Bienewski and Czyzak[9] using the form

$$n(\omega) \cong \frac{\sum_{n=0}^{N} a_n \omega^{2n}}{1 + \sum_{m=1}^{M} b_m \omega^{2m}} \quad . \tag{5.1}$$

The method used to fit a set of data points

$$\{x_i, y_i\}; \; i = 1,2,\ldots, I$$

by

$$y_i \approx \hat{y}_i = \frac{\sum_{n=0}^{N} a_n x_i^n}{1 + \sum_{m=1}^{M} b_m x_i^m} \tag{5.2}$$

is derived by multiplying each side by

$$x_i^k \left[1 + \sum_m b_m x_i^m\right] ; \; k = 0, 1, 2, \ldots, N + M$$

and summing over i. This yields a set of simultaneous linear equations for the a_n and b_m:

$$\sum_{i=1}^{I}\left\{\sum_{n=0}^{N} x_i^{n+k} a_n - y_i x_i^k - \sum_{m=1}^{M} y_i x_i^{m+k}\, b_m\right\} = 0 \qquad (5.3)$$

which may be solved directly. Thus the method is far more efficienct than a direct nonlinear least-square error determination of the coefficients.

We also attempted to fit $(\text{Re } n)^2$ as $P(\omega)/Q(\omega)$ - as opposed to fitting Re n to $P(\omega^2)/Q(\omega^2)$, but the results, for the same number of parameters, were not as good.

It was found that increasing N and M in Equation (5.1) beyond 2 gave no appreciable improvement in the fit. The rms and maximum discrepancies for the N = 2, M = 2 case,

$$n(\omega) \cong \frac{a_o + a_1\omega^2 + a_2\omega^4}{1 + b_1\omega^2 + b_2\omega^4} \qquad (5.4)$$

were:

	error	
	rms	max
ZnS - extr.	0.0019	0.005
ZnS - ord.	0.0019	0.005
CdS - extr.	0.0012	0.004
CdS - ord.	0.0010	0.003

The lack of improvement for increased M and N and the generally "random" distribution of the residuals suggests that they are due principally to measurement errors. There was, however, some indication of (narrow band) impurity absorption between 0.7 and 0.8 μm in the ZnS.

The values of the coefficients that fit the four $n(\omega^2)$ functions were:

	a_o	$a_1(\text{sec}^2)$	$a_2(\text{sec}^4)$	$b_1(\text{sec}^2)$	$b_2(\text{sec}^4)$
ZnS-e	2.2743	-8.3963×10^{-32}	7.3132×10^{-64}	-4.0365×10^{-32}	3.9840×10^{-64}
ZnS-o	2.2716	-9.3590×10^{-32}	9.3463×10^{-64}	-4.4531×10^{-32}	4.9478×10^{-64}
CdS-e	2.2921	-1.7755×10^{-31}	2.1257×10^{-63}	-8.4068×10^{-32}	1.3055×10^{-63}
CdS-o	2.2763	-1.8735×10^{-31}	2.5311×10^{-63}	-8.8744×10^{-32}	1.5003×10^{-63}

with $\omega = 2\pi c/\lambda$.

The ratio of a fit quadratic in ω^2 is equivalent to a "two oscillator" model:

$$n(\omega) \cong \frac{a_o + a_1\omega^2 + a_2\omega^4}{1 + b_1\omega^2 + b_2\omega^4} = e + \frac{f_1}{\omega_1^2 - \omega^2} + \frac{f_2}{\omega_2^2 - \omega^2} \quad , \qquad (5.5)$$

where

$$e = \frac{a_2}{b_2}$$

$$\omega_{1,2}^2 = \frac{1}{2b_2}\left[-b_1 \pm \sqrt{b_1^2 - 4b_2}\right]$$

$$f_{1,2} = -\frac{\left(a_o - \frac{a_2}{b_2}\right) + \left(a_1 - \frac{a_2 b_1}{b_2}\right)\omega_{1,2}^2}{b_1 + 2b_2\omega_{1,2}^2} \quad .$$

The values of e, $f_{1,2}$, and $\omega_{1,2}$ thus obtained were:

	e	$f_1(\text{sec}^{-2})$	$\omega_1(\text{sec}^{-1})$	$f_2(\text{sec}^{-2})$	$\omega_2(\text{sec}^{-1})$
ZnS-e	1.8356	2.1402×10^{30}	6.5697×10^{15}	2.2631×10^{31}	7.6261×10^{15}
ZnS-o	1.8890	-1.2677×10^{31}	6.5589×10^{15}	3.823×10^{31}	6.8544×10^{15}
CdS-e	1.6283	5.4890×10^{29}	3.9680×10^{15}	3.0601×10^{31}	6.9751×10^{15}
CdS-o	1.6870	1.5148×10^{31}	3.8920×10^{15}	2.4639×10^{31}	6.6335×10^{15}

The negative value for f_1 of ZnS-o is puzzling, since it has no obvious physic meaning.

Lacking any guidance from first principles on how to interpolate the data from CdS and ZnS to estimate the refractive properties of $Zn_{1-x}Cs_xS$, we tried four approaches: (1) interpolation of e, $f_{1,2}$, $\omega_{1,2}^2$, (2) interpolation of a_i, b_i, (3) interpolation of Re n, and (4) interpolation of $(\text{Re } n)^2$. (By "interpolation" we mean linear interpolation: $Q_x = xQ_{CdS} + (1 - x)\, Q_{ZnS}$.) Interpolation of the oscillator (method (1)), which we had anticipated would be a plausible approach, gave

poor results. Specifically, the iso-index point was "sucked" into the absorption region (near ω_1) for values of x very near unity. Interpolation of the coefficients a_i, b_i did give results that were at least believable. The iso-index point decreased in wavelength with decreasing x, crossing into the absorption region, however, at x = 0.76, $\lambda \cong 4340$ Å. An iso-index wavelength of 4800 Å, for example, was predicted for x ≈ 0.83. (In the approach of Section 4, an iso-index wavelength of 4800 Å requires x ≈ 0.80, as indicated by Figure 7.) Interpolation of Re n and $(\text{Re } n)^2$ gave results similar to each other, with the slope $d\lambda_{iso}/dx$ again positive, but much smaller than that of method (2).

The results obtained by method (2) are given in Figure 8. Included in Figure 8(a) for clarification are the two lower frequency poles of Equation (5.4). It is seen that the iso-index wavelength crosses into the absorption region near x = 0.76, as mentioned above. As a mathematical convenience, we plotted in Figure 8(b), the slope of birefringence multiplied by the wavelength at the iso-index point. The sharp increase in this slope is to be expected as the oscillator resonances are approached.

For completeness we show in Figures 9 and 10 the results of methods (3) and (4), respectively. As is seen, the variation of λ_{iso} with composition x is much more gradual by this method than by either method (2) above or the approach of Section 4.

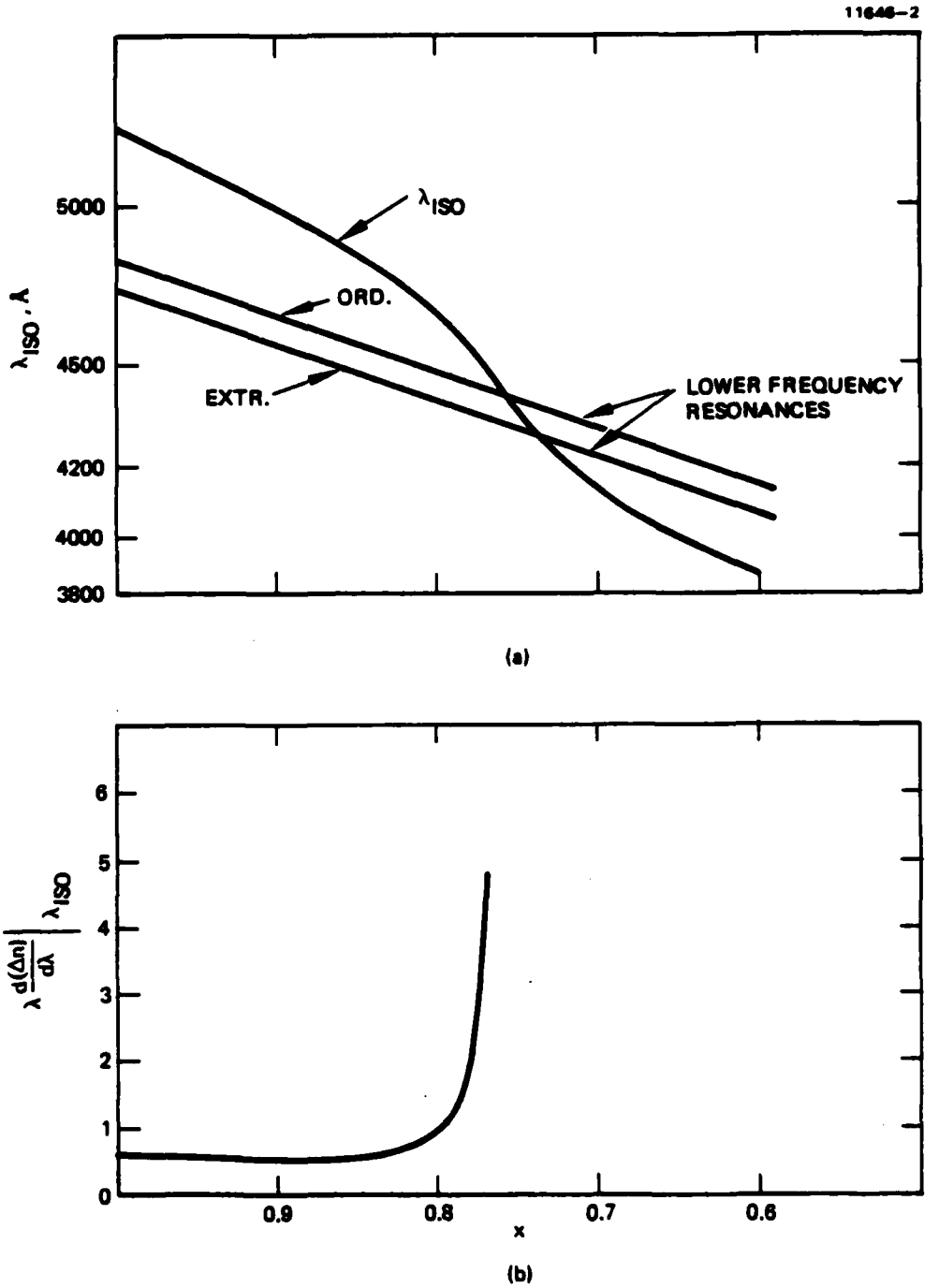

Figure 8. Dispersion characteristics of $Zn_{1-x}Cd_xS$ as a function of composition, using interpolation of Padé coefficients. (a) Iso-index point; (b) normalized slope of birefringence. Included in (a) are the lowest frequency resonances.

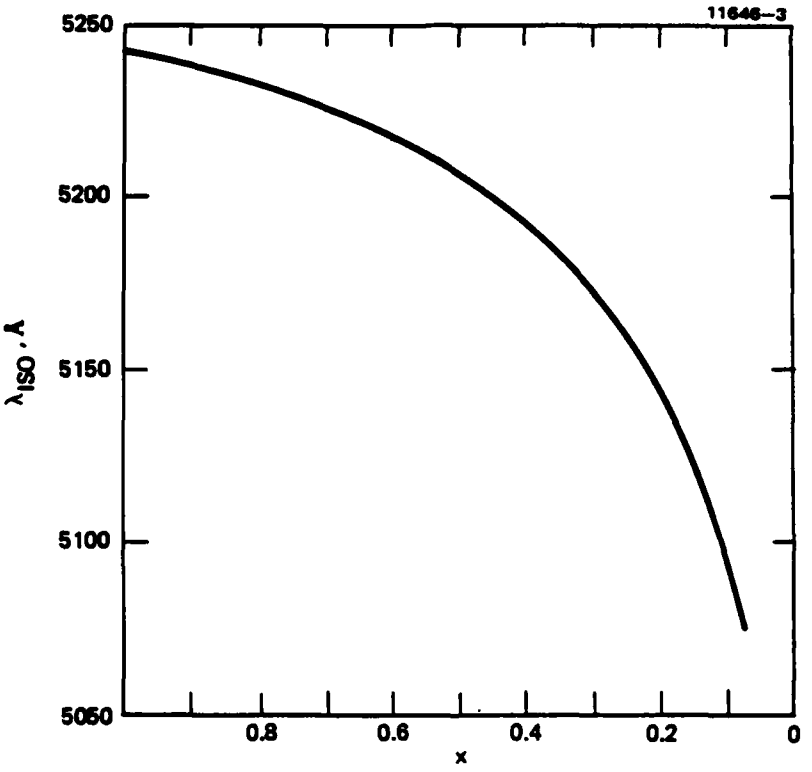

Figure 9. Iso-index point versus composition in $Zn_{1-x}Cd_xS$, using interpolation of Re n and Padé formula, Equation (5.4).

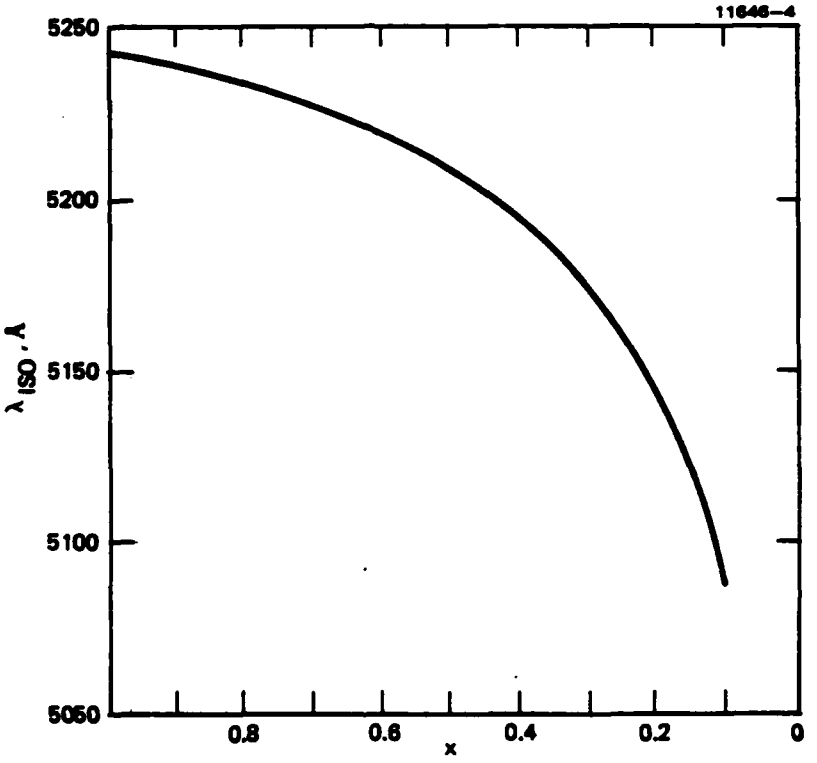

Figure 10. Iso-index point versus composition in $Zn_{1-x}Cd_xS$, using interpolation of $(\text{Re } n)^2$ and Padé formula, Equation (5.4).

SECTION 6

CONCLUSIONS

Our theoretical oscillator models of the uniaxial crystals ZnS and CdS have been shown to yield values of both ordinary and extraordinary refractive indices throughout the visible and near infrared wavelength regions with an accuracy of better than 0.5%. However, employing the theory to predict the dispersive properties of the mixed crystals $Zn_{1-x}Cd_xS$ (i.e., the iso-index wavelength and slope of birefringence) by a linear interpolation has yielded results that are only semiquantiatively in agreement with the limited experimental data available.

The following conclusions characterize the results of our study:

- The intricacies of band structure of the alloy superlattices for the mixed crystals (Zn,Cd)S are too subtle to allow accurate predictions of their refractive properties by simplified multiple classical oscilaltor models.

- Better results are obtained when $\epsilon(\omega)$ or $n^2(\omega)$, rather than $n(\omega)$, is represented by the oscillator model. Predictions of the dependence of iso-index wavelength and slope of birefringence upon Zn content are semiquantitatively correct, but only so long as we include at least two band-edge oscillator resonances in our mathematic model.

- The Padé approximation works well for $n(\omega)$, provided one interpolates directly the Padé coefficients. The model, however, yields poles coincident with the iso-index point at unexpectedly low levels of Zn concentration.

- One indicator that shows promise is that for moderate fractions of Zn, not only does the iso-index point move toward shorter wavelengths, but according to our approximate theory the slope of birefringence increases above that of pure CdS. This suggests the possibility of more highly selective iso-index filters[1] at wavelengths in the range 4600 Å to 4800 Å.

Finally, we believe that reliable experiments are needed to yield valid information on the desired dispersive characteristics of the (Zn,Cd)S alloys.

REFERENCES

1. J.F. Lotspeich, IEEE J. Quantum Electron. QE-15, 904 (1979).

2. C.H. Henry, Phys. Rev. 143, 627 (1966).

3. J.P. Laurenti, K. Rustagi, M. Rouzeyre, H. Rufer, and W. Ruppel, J. Appl. Phys. 48, 203 (1977).

4. J.L. Shay and J.H. Wernick, "Ternary Chalcopyrite Semiconductors: Growth, Electronic Properties, and Applications," p. 151, Volume 7, The Science of the Solid State, B.R. Pamplin, Editor, (Pergamon Press, New York, 1975).

5. C.W. Bunn, Chemical Crystallography, 2nd Ed. p. 87, (Clarendon Press, Oxford, 1961).

6. A.N. Winchell, Elements of Optical Mineralogy, Part I, p. 116, 5th edition; (John Wiley and Sons, New York, 1965).

7. W.M.D. Bryant, J. Am. Chem. Soc. 65, 96 (1943).

8. T.K. Bergstresser and M.L. Cohen, Phys. Rev. 164, 1069 (1967).

9. T.M. Bieniewski and S.J. Czyzak, J. Opt. Soc. Am. 53, 496 (1963).

10. See, for example, F. Stern, "Elementary Optical Properties of Solids," in Solid State Physics, F. Seitz and D. Turnbull, eds; (Academic Press, New York, 1963).

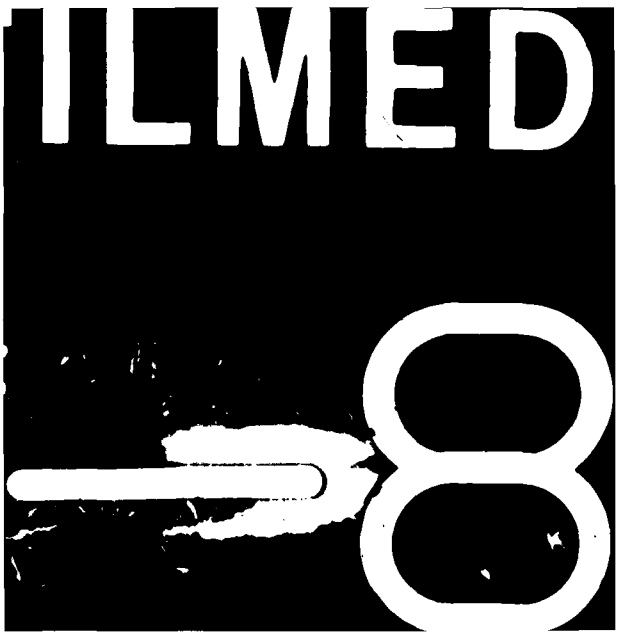
ILMED
8